

M. D. Obradović · B. N. Grgur · S. Lj. Gojković ·
Lj. M. Vračar

Enhancement of the electrochemical reduction of oxygen at platinum by nickel underpotential deposition

Received: 9 May 2005 / Revised: 16 August 2005 / Accepted: 24 August 2005 / Published online: 3 November 2005
© Springer-Verlag 2005

Abstract Polycrystalline Pt electrode was modified by underpotential deposition (upd) of nickel. The modification was performed by potential cycling in phosphate buffer pH 7.0 containing NiSO_4 , in which hydrogen and nickel upd processes were well separated. The maximum Ni upd coverage was found to be 0.3. Oxygen reduction was studied at bare and nickel upd-modified Pt. It was found that the reaction rate increased with increasing Ni upd coverage. At $\theta(\text{Ni})=0.3$, the current density was a factor of 2 higher compared to bare Pt (at the potential of 0.85 V). The capacitance of the electrode interface was determined in potential-relaxation experiments following interruption of the polarization current. It was found that the pseudocapacitance owing to a coverage by the adsorbed reaction intermediates was higher on the Ni-modified Pt surface than on bare Pt, which resulted in higher reaction rate. The influence of Ni adatoms on the surface coverage by the reaction intermediates was attributed to the inhibition of OH adsorption on Pt by OH ligands attached on neighboring Ni atoms.

Keywords Underpotential deposition · Nickel · Platinum · Oxygen reduction · Open-circuit potential-relaxation method

M. D. Obradović
Institute of Chemistry,
Technology and Metallurgy,
University of Belgrade,
Njegoševa 12,
P.O. Box 473, 11000 Belgrade,
Serbia and Montenegro

B. N. Grgur · S. Lj. Gojković (✉) · Lj. M. Vračar
Faculty of Technology and Metallurgy,
University of Belgrade,
Karnegijeva 4,
P.O. Box 3503, 11000 Belgrade,
Serbia and Montenegro
e-mail: sgojkovic@tmf.bg.ac.yu
Tel.: +381-11-3303753
Fax: +381-11-3370387

Introduction

The electrochemical oxygen reduction continues to attract considerable attention because of its role in electrochemical energy conversion, several industrial processes, and corrosion. This reaction is also interesting from fundamental point of view because of its complex mechanism and sensitivity to the structural and electronic properties of the electrode surface [1, 2].

Despite an extensive research work in finding low-cost electrocatalyst, platinum is still the only single-metal electrode material that can fulfill demands in fuel cells working in acid media. However, numerous studies reported that Pt alloys (mostly with transition metals as Co, Ni, Cr, and Fe) are more active for oxygen reduction than pure Pt [3–12]. Some of the studies were performed with carbon-supported alloys [3, 4, 8, 10, 11], while the others investigated sputtered alloy films [5–7] or metallurgically prepared bulk alloys [9, 11, 12]. The enhancement of the oxygen reduction rate was ascribed to the three effects and their interplay: the change in Pt–Pt bond distance [3, 4, 8], the modification of the 5-d orbital vacancies of Pt atoms [4–7, 9, 12], and the change of the adsorption properties of OH species at Pt atoms neighboring transition metal atom [10, 11]. The increase in the reaction rate with the decreasing Pt–Pt distance due to contraction of face-centered cubic (fcc) lattice during alloying was well documented [3, 8] and rationalized by favored geometry for rupture of the O–O bond. On the other hand, increase in the oxygen reduction rate was also observed at the alloys which outermost layer was pure Pt (“skin” structure) [5–7, 9]. Since geometric effects had to be ruled out in that case, it was postulated that the nature of the oxide formed on Pt-skin atoms was changed because of the electronic modification by transition metal atoms in the layer underneath [9]. Adsorption of OH species on Pt atoms could be changed also by the OH ligands attached to the alloying atoms when they are stable on the surface during oxygen reduction [11].

The simple way to produce a bimetallic surface with the precise and deliberate control of the surface coverage is

underpotential deposition (upd) of a foreign metal on a substrate. Metal adatoms are believed to have electronic properties different from those of the bulk material as well as electronic properties of the substrate can be altered by the adatoms [13]. Owing to such characteristics, metal surfaces modified by upd of other metals are widely used in research in electrocatalysis.

Oxygen reduction was investigated at Au modified by upd of Pb [14], Tl [15], Ag [16], etc., and a significant catalytic effect was observed. It was found that the effect was due to facilitated H₂O₂ reduction, meaning that foreign metal adatoms transformed Au as a two-electron reducer into four-electron reducer. Oppositely, when Pt surface, which is four-electron reducer, was modified by upd of Cu [17], Pb [18], and Sn [19], oxygen reduction was inhibited by promoting two-electron reduction. However, there was no attempt to test oxygen reduction at Pt surface modified by upd of transition metals.

In the present study, we chose Ni as metal that enhanced oxygen reduction rate in both bulk Pt₃Ni alloys [9] and in the carbon supported Pt₃Ni nanoparticles [10]. Polycrystalline Pt surface was modified by upd of Ni, and oxygen reduction was studied on such an electrocatalyst. Adsorption characteristics of bare and modified Pt were investigated to explain the effect of Ni on the kinetics of the reaction.

Experimental

Polycrystalline platinum electrode with the diameter of 3 mm in the form of rotating disk (Tacussel) was used in this study. Before the deposition of Ni, the electrode was polished with an aqueous suspension of Al₂O₃ of the grain sizes of 1, 0.5, and 0.3 μm and washed by high-purity water in an ultrasonic bath. A large-area platinum gauze counter electrode and a saturated calomel electrode (for Ni deposition), or reversible hydrogen electrode (RHE) (for oxygen reduction) as the reference electrode, were employed. All the potentials are expressed on the scale of RHE. The cell was thermostated at 25°C.

All the solutions were prepared with *pro analysi* grade chemicals (Merck): NiSO₄, NaH₂PO₄, and NaOH and high purity water (Millipore, 18 MΩ cm) whose cleanliness was checked by recording cyclic voltammogram at Pt electrode and comparing it with the same in the literature [20]. The solutions were purged with nitrogen (for Ni deposition) or oxygen (for oxygen reduction) and kept under these atmosphere throughout the duration of the experiments.

Underpotential deposition of Ni was performed by linear sweep at the rate of 50 mV s⁻¹ in the phosphate buffer solutions of pH 7.0 (0.10 mol dm⁻³ NaH₂PO₄+0.10 mol dm⁻³ NaOH) containing 1.0×10⁻⁵ to 1.0×10⁻³ mol dm⁻³ NiSO₄. The electrode was rotated at 1,000 rpm. Roughness factor of the Pt surface was determined from the steady-state cyclic voltammogram recorded in the phosphate buffer solution. After correction of the hydrogen desorption charge for the double-layer charging, and assuming a charge of 210 μC cm⁻² for monolayer hydrogen adsorption, a roughness factor of 1.8±0.1 was estimated. Oxygen

reduction was investigated in 0.10 mol dm⁻³ NaOH solution. Polarization curves were recorded at the rotation rate of 1,600 rpm by linear sweep of 20 mV s⁻¹ going from the limiting current plateau to the open-circuit potential. Potentiostat EG&G PAR Model 371, PAR Universal Programmer Model 175, and X-Y recorder Philips PM 8143 were used for the polarization measurements.

The potential-relaxation measurements were taken from a cathodic potential of 0.7 V by interruption of the polarizing current using a very fast electric switch. The data were digitally collected by a PC computer connected to the potentiostat. A home-made software for data processing was employed.

Results and discussion

Modification of Pt by nickel upd

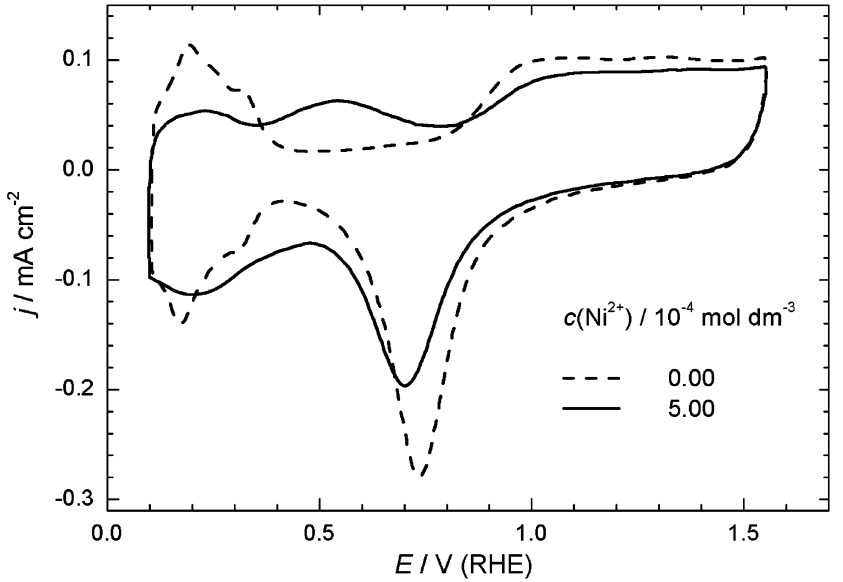
Underpotential deposition of metal adatoms on Pt surface is always competitive with hydrogen adsorption. Therefore, to determine surface coverage by metal adatoms, this upd process must not overlap with hydrogen adsorption/desorption region. El-Shafei [21] demonstrated that in strong acid media, the Ni upd occurred within the hydrogen adsorption/desorption region, but in phosphate buffer of pH of about 7, these processes were well separated [22]. Therefore, we modified the Pt surface in phosphate buffer of pH 7.0. After the steady-state voltammogram of Pt was obtained, solution of NiSO₄ was added into the electrolyte, and the linear potential sweep was continued. In the presence of Ni²⁺ ions, the negative potential limit was set to be more positive than the Ni²⁺/Ni reversible potential to prevent overpotential deposition. The voltammograms of Pt in the electrolyte without and with Ni²⁺ are given in Fig. 1. After several cycles, which were stable during time, the positive potential limit was set to 0.85 V to avoid formation of Pt oxide and overlapping its reduction with deposition of Ni and adsorption of hydrogen. The voltammograms in the electrolytes containing different concentration of Ni²⁺ ions are presented in Fig. 2.

Anodic peaks at about 0.5 V (Fig. 2) originate from the dissolution of Ni. When the dependence of the peak potential was plotted as a function of the concentration of Ni²⁺ ions, a straight line with the slope of 33 mV dec⁻¹ was obtained (inset in Fig. 3). This result shows that upd of Ni proceeds with the transfer of two electrons and that Ni is deposited as a neutral atom.

From the voltammograms given in Fig. 2, the cathodic charge for both deposition of Ni and adsorption of hydrogen and the anodic charge for desorption of hydrogen were determined. The difference between the cathodic and the anodic charge was ascribed to the nickel deposition, $Q(Ni)$, and the surface coverage was calculated according to

$$\theta(Ni) = \frac{Q(Ni)}{2 \cdot h \cdot 210 \mu C cm^{-2}} \quad (1)$$

Fig. 1 Stationary cyclic voltammograms of Pt electrode in phosphate buffer solution pH 7.0 without and with Ni^{2+} ions. Sweep rate 50 mV s^{-1} , rotation rate 1,000 rpm



where h is the roughness factor of the electrode. The $Q(\text{Ni})$ and $\theta(\text{Ni})$ values were also determined by the integration of the anodic peak of Ni oxidation. These two methods gave similar results, and their arithmetic mean was used as a true value of the surface coverage. Fig. 3 presents the dependence of the Ni upd coverage on the concentration of Ni^{2+} ions in the electrolyte. The coverage approaches a limiting value of 0.30 at $5.0 \times 10^{-4} \text{ mol dm}^{-3} \text{ Ni}^{2+}$. The limiting value is half of the maximal surface coverage attained in the work of El-Shafei [21], which is probably an effect of anion, i.e., we used NiSO_4 , while El-Shafei [21] used NiClO_4 .

Oxygen reduction kinetics

After several cycles in Ni^{2+} containing phosphate buffer, the potential of the Pt electrode was held at the negative

limit, and the electrode was taken out from the electrolyte, washed out by water, and, under potentiostatic control ($E=0.1 \text{ V}$), immersed into another cell filled with oxygen-saturated NaOH solution. Then a polarization curve for oxygen reduction was recorded in a positive going sweep toward open-circuit potential at a sweep rate of 20 mV s^{-1} . In a separate experiment, the background current was determined in N_2 -saturated NaOH solution under the same conditions. The polarization curve and the background current were also measured at bare Pt surface. The results for bare Pt and the Pt surface modified by Ni upd of $\theta=0.3$ are given in Fig. 4. They represent mean values of five repeat experiments, each of them performed on freshly prepared electrode surface.

The background current at the modified Pt electrode shows a decrease in the hydrogen desorption charge and a broad peak of oxidation of Ni adatoms that overlap the Pt-oxide formation, evidencing that Ni adatoms had not been

Fig. 2 Stationary cyclic voltammograms of Pt electrode in phosphate buffer solution pH 7.0 containing different concentration of Ni^{2+} ions. Sweep rate 50 mV s^{-1} , rotation rate 1,000 rpm

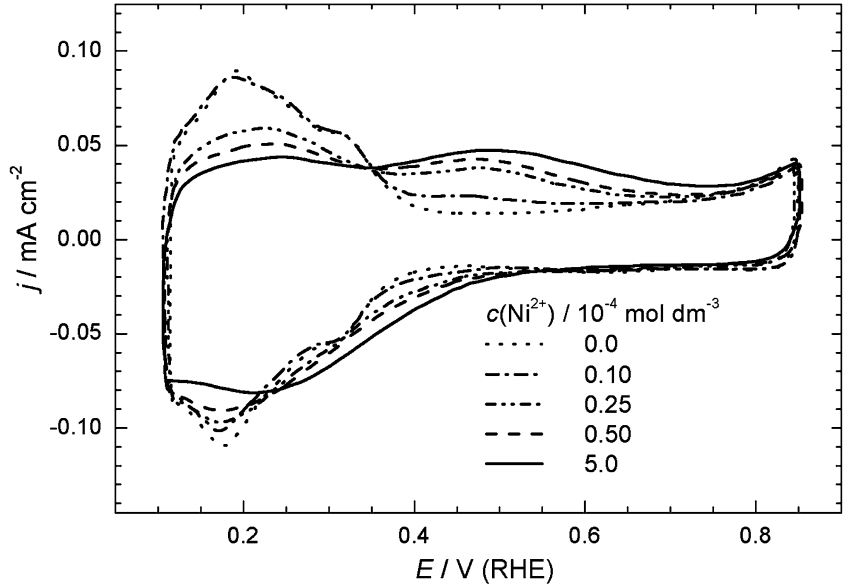
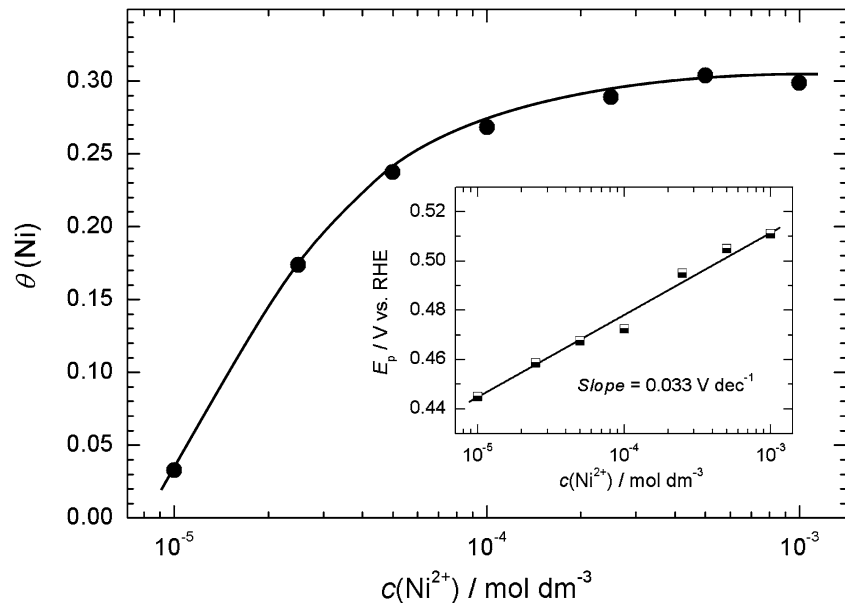


Fig. 3 Surface coverage of Pt surface by upd Ni as a function of Ni^{2+} concentration. Inset: variation of the potential of the Ni upd desorption peak with the concentration of Ni^{2+} in phosphate buffer pH 7.0



removed during the transfer from one cell to another. After subtracting the background current from the polarization curves recorded in the oxygen-saturated solution, the true oxygen reduction current densities were obtained. This correction was significant only at the potentials very close to the open-circuit potential (up to 0.9 V). The corrected polarization curves showed, like those in Fig. 4, that the limiting current densities for oxygen reduction were the same at both Pt surfaces, but at lower overpotentials, the higher reaction rate at the Ni-modified Pt was evident.

The Tafel plots for oxygen reduction on bare Pt and Pt modified by different amounts of Ni adatoms are given in Fig. 5. The current densities were corrected for the diffusion effects assuming first-order kinetics with respect to dissolved oxygen [23] and using the equation [24]

$$j_k = \frac{j \cdot j_L}{j_L - j} \quad (2)$$

where j_k is the kinetic current density, j is the measured current density, and j_L is the limiting current density. At low current densities, the slope is slightly dependent on the surface coverage by Ni, and its value was about -60 mV dec^{-1} . At high current densities, the Tafel slope was about -120 mV dec^{-1} . The influence of Ni adatoms is more expressed at the high current densities. At 0.85 V, what is usually taken as a reference potential for a comparison of the catalysts regarding oxygen reduction rate, the platinum surface with $\theta(\text{Ni})=0.3$, is two times more active than pure Pt. The activity enhancement of factor 2 is the same as in the study of oxygen reduction at the Pt_3Ni bulk alloy in acid media [9].

Since the Tafel slopes for oxygen reduction at bare and Pt modified by upd of Ni are essentially identical, the mechanism of the reaction on both surfaces is probably the same. This was also concluded for Pt_3Ni and Pt_3Co alloys in acid media [9–12] and Pt_3Co alloys in alkaline media

[25]. Activity enhancement of oxygen reduction at Pt by transition metal atoms was explained in the literature [9–12] by the changes in ability of Pt to adsorb OH species. This can be caused by the altering of electronic structure of Pt that was proved in the case of “skin” Pt structure [9, 12] where transition metal atoms are not present on the surface

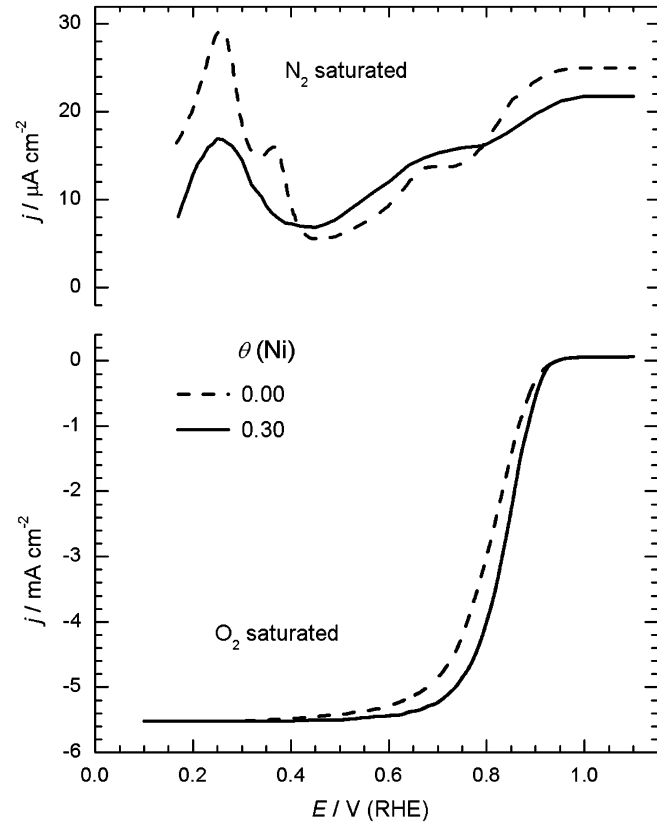
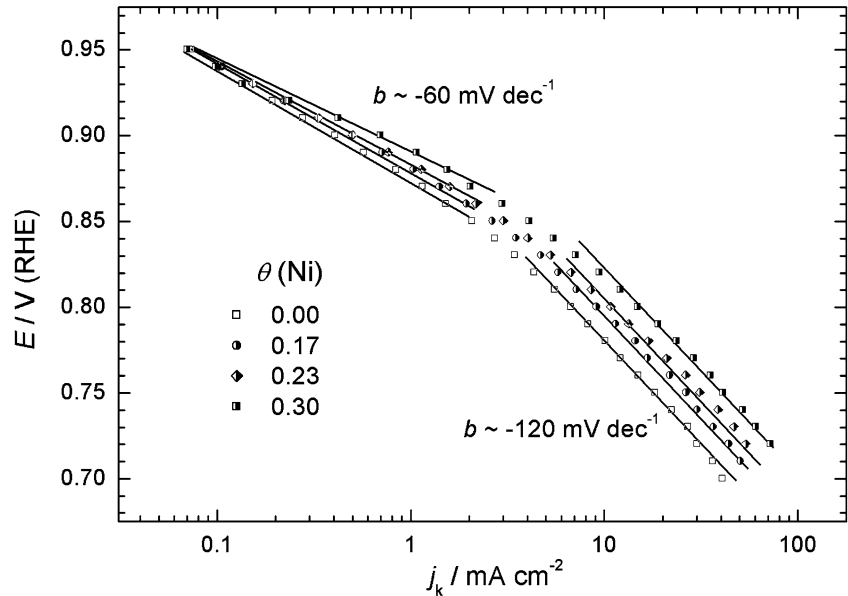


Fig. 4 Background currents (upper diagram) and polarization curves in oxygen saturated electrolyte (lower diagram) at bare and Ni upd-modified Pt surface [$\theta(\text{Ni})=0.3$] recorded in 0.1 mol dm^{-3} NaOH . Sweep rate 20 mV s^{-1} , rotation rate 1,600 rpm

Fig. 5 Tafel plots for oxygen reduction recorded in 0.10 mol dm⁻³ NaOH at bare and modified Pt surfaces with different coverage of Ni upd. Sweep rate 20 mV s⁻¹, rotation rate 1,600 rpm. Current densities corrected for diffusion effects



of the electrocatalyst. When both Pt and transition metal atoms are exposed to the solution, the latter ones are likely to have one or more OH ligands attached. The presence of OH species on the foreign atoms could hinder the formation of oxide on the neighboring Pt [10, 11]. To find out whether Ni adatoms influences the adsorption characteristics of Pt, pseudocapacitance of the pure and modified Pt was determined.

Potential-relaxation behavior

The analysis of the potential-relaxation behavior of an electrode reaction, following interruption of the polarization current, provides information on capacitance behavior of the electrode interface and on the kinetics and mechanism of the electrochemical reaction [26, 27]. The open-

circuit potential-relaxation approach was successfully applied in the analysis of oxygen reduction [28].

When the polarization is interrupted from a potential in the Tafel region, the following relationship between potential and time during relaxation is valid [26–28]:

$$(C_{dl} + C_\phi) \cdot \frac{d\eta}{dt} = j(\eta) = j_0 \exp\left(-\frac{\alpha_c F \eta(t)}{RT}\right) \quad (3)$$

where C_{dl} is the double-layer capacitance of the electrode interface, C_ϕ is the pseudocapacitance associated with potential dependence of coverage by the intermediates, η is overpotential of the reaction, and $j(\eta)$ is the current density measured as a function of overpotential (Tafel relation), determined experimentally under the same conditions as employed for the recording of the $E(t)$ transient. If C_{dl} and C_ϕ behave as though they are connected in parallel, the

Fig. 6 Potential-relaxation plot for oxygen reduction at bare and Ni upd-modified Pt surface [$\theta(\text{Ni})=0.3$] recorded in 0.10 mol dm⁻³ NaOH. Polarization current interrupted at 0.7 V

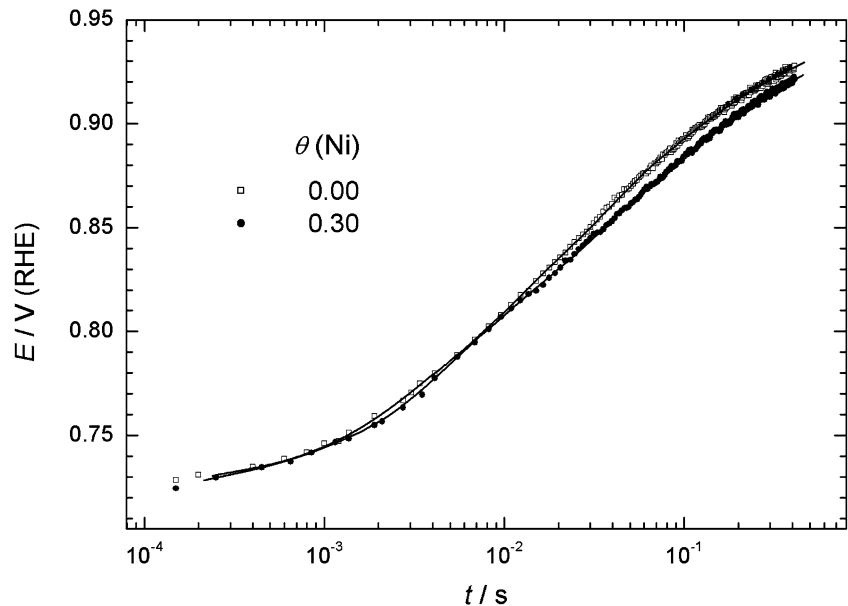
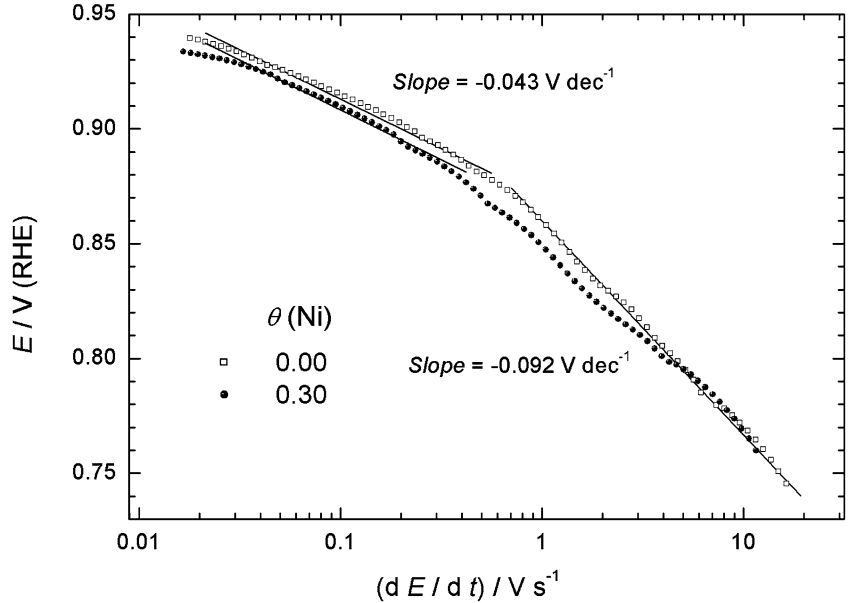


Fig. 7 Plots E vs $\log(dE/dt)$. Data taken from Fig. 6



total capacitance, C , is $C=C_{dl}+C_\phi$. After taking logarithm of the Eq. 3, then replacing overpotential by potential, and solving the equation by the potential, one obtains [27]:

$$E = E_{eq} + b \log j_o - b \log C(E) - b \log \left(\frac{dE}{dt} \right) \quad (4)$$

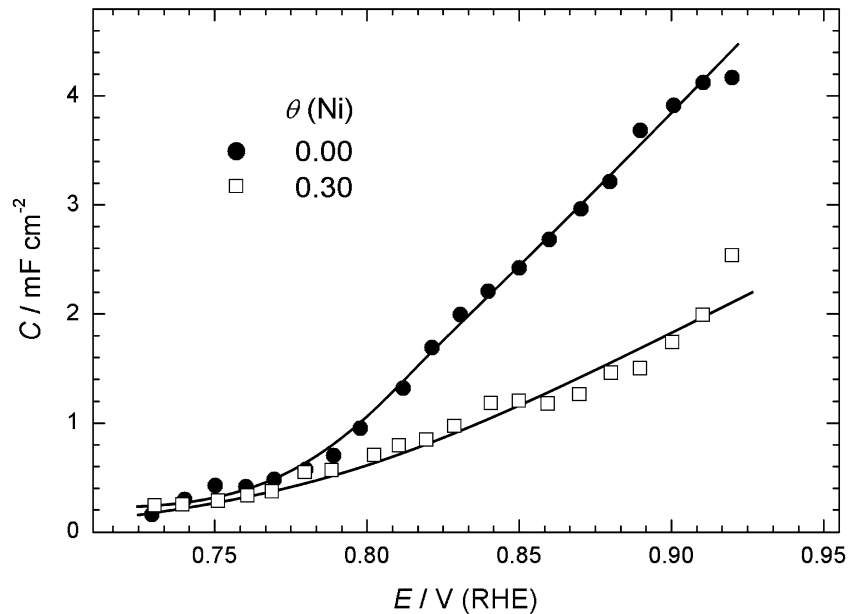
where E_{eq} is equilibrium potential of the reaction, and b is the Tafel slope. The linearity and the slope of E vs $\log(dE/dt)$ graph equal to the Tafel slope is an indication that the capacitance does not depend on the potential. If this is not the case, the capacitance is to be determined using dE/dt and $j(E)$ data (see Eq. 3).

The open-circuit potential-relaxation curves were recorded under the same conditions as the polarization curves. After having immersed the electrode into the oxygen-saturated

electrolyte and swept the potential to 0.7 V, the electric circuit was interrupted, and the potential vs time data were collected. The results for bare Pt and Pt modified by Ni adatoms are presented in Fig. 6. The processed data in the form of E vs $\log(dE/dt)$, given in Fig. 7, show that the curves at low overpotentials can be approximated by the lines with the slope of about -45 mV dec $^{-1}$, while at high overpotentials the slope is about -90 mV dec $^{-1}$. The difference between the slopes in Fig. 7 and the Tafel slopes in Fig. 5 suggests that the total capacitance depends on the potential. Therefore, potential-dependent capacitance values were determined according to Eq. 3:

$$C = \frac{j(E)}{(dE/dt)} \quad (5)$$

Fig. 8 Potential-dependent capacitance of bare and Ni upd-modified Pt surface [$\theta(Ni)=0.3$] in the course of oxygen reduction in 0.10 mol dm $^{-3}$ NaOH. Capacitances calculated using data from Figs. 4 and 7



by combining $j(E)$ data from Fig. 4 and dE/dt from Fig. 7 for the same E value.

On the plot of the potential-dependent capacitance for bare and modified Pt surfaces (Fig. 8), two regions can be distinguished. In the potential region corresponding to high overpotentials, where the potential relaxation occurs mainly through the discharge of C_{dl} at the electrode-solution interface, the capacitances for both surfaces are close to each other and independent on the potential. However, at low overpotentials where the potential is relaxed mainly through C_ϕ , an approximately linear dependence of the capacitance on the potential is observed. In this region, Pt-modified surface features significantly higher capacitance than bare Pt. This points out a higher surface coverage by the adsorbed intermediates at the modified Pt electrode.

It is not likely that Ni atoms act as the active sites for oxygen reduction, because Pt is much more active for this reaction than Ni. Therefore, higher surface coverage of Pt atoms by the reaction intermediates is to be responsible for the enhanced reaction rate on the modified Pt surface. Bearing in mind that the mechanism of the reaction on modified Pt is probably the same as on bare Pt, the higher surface coverage by the reaction intermediates should originate from the lower coverage by OH_{ads} . The hindered formation of OH_{ads} in the presence of neighboring Ni atoms was proposed by Paulus et al. [10, 11]. In our experiments, this effect is also evidenced from the cyclic voltammograms of bare and modified Pt (Figs. 1 and 4), in which formation of Pt-oxide is shifted toward more positive potentials at the Ni upd-modified electrode.

Conclusions

From the study of Ni upd at Pt surface and the effect of the surface modification on the oxygen reduction kinetics, the following can be concluded:

- Underpotential deposition of Ni at Pt was successfully performed from the phosphate buffer solution of pH 7.0 in which surface coverage by Ni adatoms can be determined precisely.
- The oxygen reduction rate increased with increasing surface coverage by Ni adatoms. At $\theta(\text{Ni})=0.3$, the current density was a factor of 2 higher compared to bare Pt (at the potential of 0.85 V).
- The similarity of the Tafel slopes for bare and modified Pt indicated the same reaction mechanism.
- The pseudocapacitance owing to a coverage by the adsorbed reaction intermediates was found to be higher on the Ni-modified Pt surface than on bare Pt, which was in agreement with the enhanced oxygen reduction current density.
- The influence of Ni adatoms on the surface coverage by the reaction intermediates was ascribed to the inhibition of OH adsorption on Pt by OH ligands attached on neighboring Ni atoms.

- The results on the influence of a transition metal on the activity of Pt regarding oxygen reduction obtained by upd modification of the Pt surface were consistent to those obtained at bulk alloys. This demonstrated that upd-modified Pt surface can be used for a fast test of a potential promoter of the oxygen reduction.

Acknowledgement This work was supported financially by the Ministry of Science and Environmental Protection of the Republic of Serbia, Contract No. H-1796.

Reference

1. Kinoshita K (1992) Electrochemical oxygen technology. Wiley, New York
2. Adžić R (1998) Recent advances in the kinetics of oxygen reduction. In: J. Lipkowski, Ross PN (eds) Electrocatalysis, Wiley, New York
3. Jalan V, Taylor EJ (1983) *J Electrochem Soc* 130:2299
4. Mukerjee S, Srinivasan S, Soriaga MP (1995) *J Electrochem Soc* 142:1409
5. Toda T, Igarashi H, Watanabe M (1998) *J Electrochem Soc* 145:4185
6. Toda T, Igarashi H, Uchida H, Watanabe M (1999) *J Electrochem Soc* 146:3750
7. Toda T, Igarashi H, Watanabe M (1999) *J Electroanal Chem* 460:258
8. Min M, Cho J, Cho K, Kim H (2000) *Electrochim Acta* 45:4211
9. Stamenković V, Schmidt TJ, Ross PN, Marković NM (2002) *J Phys Chem B* 106:11970
10. Paulus UA, Wokaun A, Scherer GG, Schmidt TJ, Stamenkovic V, Radmilovic V, Markovic NM, Ross PN (2002) *J Phys Chem B* 106:4181
11. Paulus UA, Wokaun A, Scherer GG, Schmidt TJ, Stamenkovic V, Markovic NM, Ross PN (2002) *Electrochim Acta* 47:3787
12. Stamenković V, Schmidt TJ, Ross PN, Marković NM (2003) *J Electroanal Chem* 554–555:191
13. Herrero E, Buller LJ, Abruña HD (2001) *Chem Rev* 101:1897
14. Adžić RR, Tripković AV, Marković NM (1980) *J Electroanal Chem* 114:37
15. Adzic RR, Wang JX (1996) Atomic structure of active sites in O_2 reduction on Au(111)/Tl_{ad} electrodes in acid and alkaline solutions. In: Adzic RR, Anson FC, Kinoshita K (eds) Oxygen electrochemistry, vol. 95–26. The Electrochemical Society, Pennington
16. Kongkanand A, Kuwabata S (2003) *Electrochem Commun* 5:133
17. Abe T, Swain GM, Sashikata K, Itaya K (1995) *J Electroanal Chem* 382:73
18. Machado SAS, Tanaka AA, Gonzales ER (1994) *Electrochim Acta* 39:2591
19. Zinola CF, Rodríguez J (2002) *J Solid State Electrochem* 6:412
20. Conway BE, Sharp AWB, Angerstein-Kozlowska H, Criddle EE (1973) *Anal Chem* 41:1321
21. El-Shafei AA (1998) *J Electroanal Chem* 447:81
22. Obradović MD, Grgur BN, Vračar LjM (2005) *Mater Sci Forum* 494:241
23. Damjanovic A, Brusic V (1967) *Electrochim Acta* 12:615
24. Gileadi E (1993) *Electrode kinetics*. VCH, New York, p 5
25. Obradović MD, Grgur BN, Vračar LjM (2003) *J Electroanal Chem* 548:69
26. Conway BE, Bourgault PL (1962) *Trans Faraday Soc* 58:593
27. Conway BE, Bai L, Tessier DF (1984) *J Electroanal Chem* 161:39
28. Vračar Lj, Conway BE (1990) *Electrochim Acta* 35:1919